March - April 2020
ISSN: 0193-4120 Page No. 4547 - 4556

Process Parameter Optimization of EPDM Grommet for the Implementation of Airjet Insertion

Ha-Neul Lee[1], Young-Shin Kim[2], Euy-Sik Jeon[*3]

[1]Student, Department of Mechanical Engineering, Kongju National University, 31080, Korea.
[2]Research Professor, Mechanical Engineering, Industrial Technology Research Institute, Kongju National University, 31080, Korea.
[*3]Professor, Department of Mechanical Engineering, Industrial Technology Research Institute, Kongju National University, 31080, Korea.
A20190104@smail.kongju.ac.kr[1], people9318@kongju.ac.kr[2], osjun@kongju.ac.kr[*3]

Article Info
Volume 83
Page Number: 4547 - 4556
Publication Issue:
March - April 2020

Abstract

Background/Objectives: This study investigated the process parameter optimization for parameters such as the process temperature, process time, and internal diameter of EPDM rubber grommet for an eco-friendly airjet insertion method that does not use adhesive to fix the grommet, a rubber product protecting cables from the in-vehicle frame. The adhesive hardens with time and loses its holding power; moreover, volatile organic compounds may be generated.

Methods/Statistical analysis: Tensile strength and elongation percentage tests were conducted to determine the effects of process temperature and process time on the elastic force. Subsequently, insertion force and separation force experiments were conducted to optimize the process temperature, process time, and internal diameter, which affect the structural properties of the grommet. Grommet specimens were fabricated with three different values each for the process temperature, process time, and internal diameter and the experiments were performed with 27 grommet specimens.

Findings: Based on the experimental data, we analyzed the parameters affecting the insertion and separation forces through the full factorial design of the design of experiment and derived the optimized process parameters and internal diameter values according to the optimization target criteria.

Improvements/Applications: Therefore, the purpose of the proposed airjet insertion method is to hold the cable in place using only the elastic force of the rubber without using adhesive.

Article History
Article Received*: 24 July 2019*
Revised*: 12 September 2019*
Accepted*: 15 February 2020*
Publication*: 26 March 2020*

Keywords: *Grommet, EPDM rubber, Airjet, Process parameter, Optimization.*

1. Introduction

A grommet is a rubber product inserted through the hole of the vehicle frame to prevent damage to the cables, the in-vehicle wiring. The grommet prevents damage to the cable and simultaneously secures the cable at a desired place. A grommet of EPDM rubber is generally used as sealing material. It has superior resistance and durability, and excellent low-temperature characteristics, leading to its wide use in vehicles.

EPDM grommet is produced by injection molding at high temperatures, where process temperature and process time change the physical properties of

the raw materials. This affects the elastic force by which the grommet holds the cable in place.

Currently, various studies are being conducted on EPDM rubber, mainly regarding its reliability. Studies on various shapes [1-7] have been conducted and analyses of the physical properties by mixing materials are being conducted [8-10]. Recently, shape optimization has been performed through analyzing the physical properties of EPDM grommet [11]. However, studies investigating process parameters have been scarce.

This study examines the bonding between the grommet and cable. This bonding is generally carried out using adhesives. However, the grommet and the cable become detached from each other over time because the adhesive hardens as time passes, losing its holding power. In addition, environmentally friendly methods are required to remove volatile organic compounds generated from adhesives. Therefore, the airjet insertion method, which is an environmentally friendly method, was implemented to hold the cable in place using only the elastic force of rubber without using adhesives. The airjet insertion method involves inserting the cable efficiently by fixing the grommet to the jig that can be sealed when inserting the cable into the grommet, and temporarily inflating it by blowing air to insert the cable. For the application of the method, it is necessary to determine the insertion force, which is the pressure of the air blown into the grommet, and the separation force, which is the force that keeps the cable from being detached from the grommet. The insertion and separation forces are affected by the elastic force and the internal diameter of the EPDM grommet. In other words, if the elastic force is strong, high pneumatic pressure is required for insertion. If the elastic force is weak, the force for fixing the cable is weakened, leading to the problem of lowered separation force. Therefore, the tensile strength test and elongation percentage test were performed by applying the rubber tensile strength test (ISO 1407) method to determine the effects of process temperature, process time, and internal diameter on the insertion and separation forces. The experiment was conducted by fabricating grommet specimens with varying internal diameter. The design of experiment (DOE) program using the full factorial design used Minitab 19 and derived the optimized values for process temperature, process time, and internal diameter based on the experimental results.

2. Elastic Force Experiment and the Experiment Setup

An elastic force experiment was conducted to determine the effect of process parameters, which are the process temperature and process time, on EPDM rubber.

2.1. EPDM rubber specimen model

Tensile strength and elongation percentage were measured for the analysis of process temperature and process time, the process parameters affecting the grommet produced by the injection molding of heated rubber. The elastic force was analyzed using the elastic modulus calculated based on the results.

The specimen shown in Figure 1 was fabricated according to the rubber tensile strength test (ISO 1407) specification and dumbbell type 3 specimen was used. Within the range of injection molding, the specimens were prepared with the process temperatures of 160 ℃, 170 ℃, and 180 ℃, and the process times of 200 s, 300 s, and 400 s, resulting in nine specimens in total for the experiment.

March - April 2020
ISSN: 0193-4120 Page No. 4547 - 4556

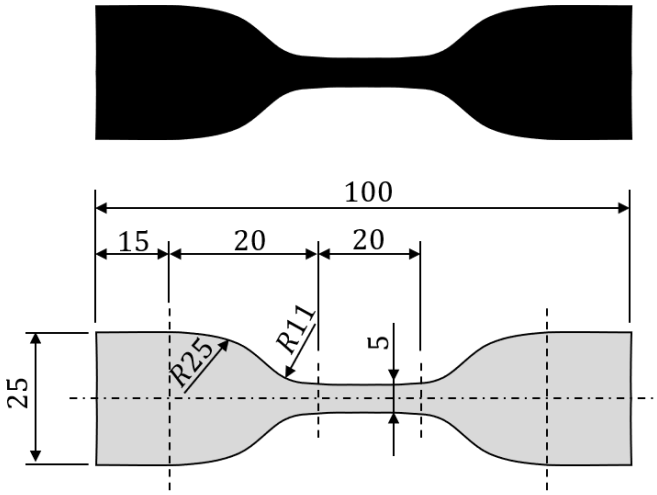

Figure 1. Specimen specification for rubber tensile strength test.

2.2. Tensile strength and elongation percentage test

Figure 2 shows the schematic diagram of the measurements in the rubber tensile strength test. The elongation percentage was measured based on the elongation percentage of 100% increase from the reference length of the specimen from the data, as the grommet is expanded with air and the expanded size is small. The test was performed at a speed of 500 mm/min. The experiment was repeated four times for each type of specimen.

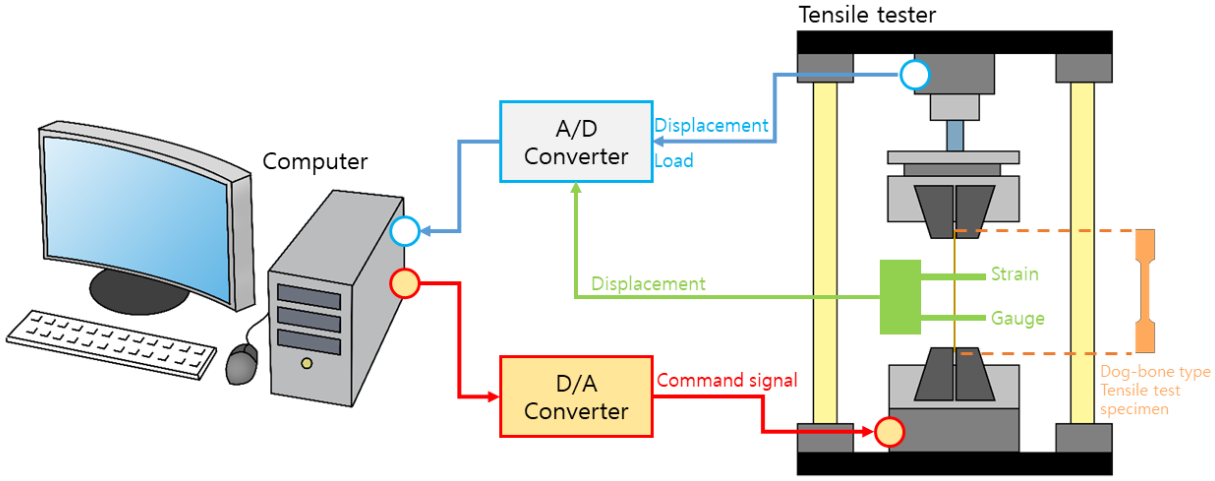

Figure 2. Schematic diagram for rubber tensile strength test.

2.3. Tensile strength and elongation percentage test

Figure 3 shows the main effects and interaction of the parameters affecting the calculated elastic modulus, which are the process temperature and process time. In Figure 3 (a), the parameters affecting the elastic modulus are divided into process temperature and process time. The process temperature had a greater effect than the process time, and the greatest effect was observed at the process temperature of 180 ℃. In addition, in Figure 3 (b), the elastic modulus is shown to be directly proportional to the process temperature and process time. As for the interaction, the process times of 300 s and 400 s showed interaction at the process temperature of 170 ℃.

March - April 2020
ISSN: 0193-4120 Page No. 4547 - 4556

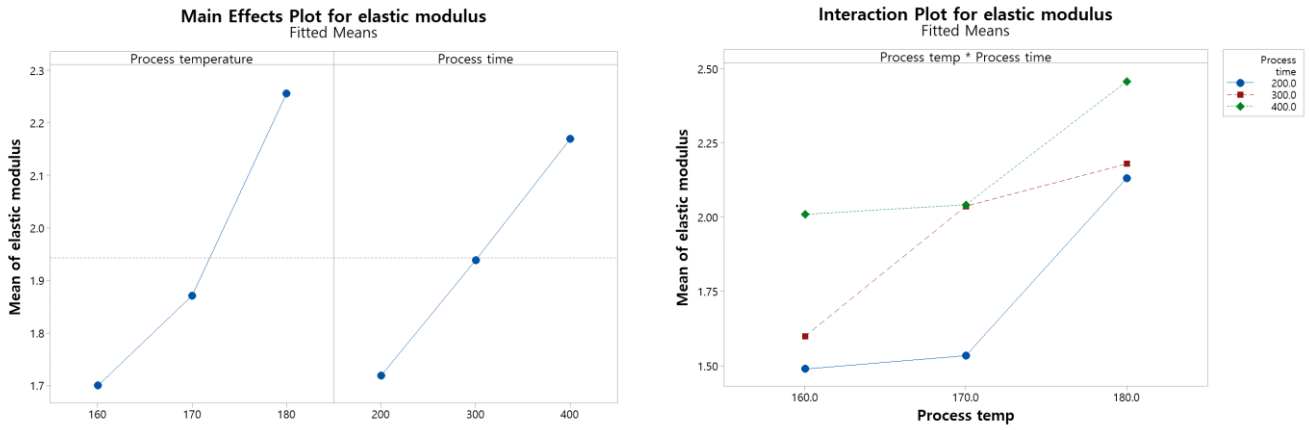

(a)Main effects plot for elastic modulus (b) Interaction plot for elastic modulus

Figure 3. Main effects plot and interaction plot for elastic modulus.

3. Insertion Force and Separation Force Measurement

The insertion force and separation force experiments were performed considering the process parameters and internal parameter, which is the structural parameter.

3.1. Experimental model

The experimental model of the grommet is shown in Figure 4. Twenty seven types of grommets were fabricated with three different values each for the process parameters and three values of internal diameter (Ain) of 3.4 mm, 3.7 mm, and 4.0 mm. As shown in Table 1, the outer diameter of the grommet (Aout) was 10 mm and the grommet length (Ah) was 24 mm, the same for all specimens. The diameter (D) of the cable was maintained at 4.4 mm and the same cable was used, with the length (C) of 200 mm.

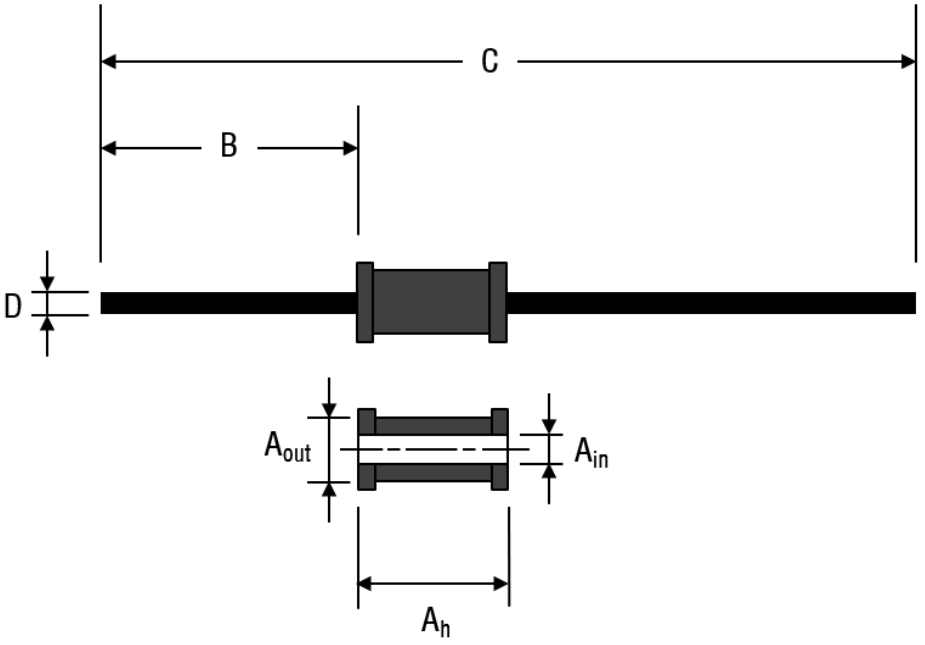

Figure 4. Grommet model.

March - April 2020
ISSN: 0193-4120 Page No. 4547 - 4556

Table 1: Grommet model size

Part		Value (mm)
	case 1	3.4
A_{in}	case 2	3.7
	case 3	4.0
A_{out}		10.0
A_h		24.0
B		76.0
C		200.0
D		4.4

3.2. Insertion force experiment

An insertion force experiment was performed by airjet insertion. As shown in Figure 4 and Table 1, the maximum pneumatic pressure was examined based on the insertion of the 100 mm cable (Ah, B). Figure 5 (a) shows the grommet and cable coupled to the actual airjet insertion equipment, and the schematic diagram shows the air supply when the cable is inserted into the grommet. Figure 5 (b) is a flowchart of the insertion force experiment, which involves increasing the air pressure to examine the air pressure when the cable is inserted. When the cable began to be inserted, the pressure increase was stopped and the maximum air pressure up to an insertion of 100 mm was measured. Four replicate experiments were performed per specimen type.

Table 2 shows the analysis of variance for the insertion force. It can be observed that the p-value of the process temperature is 0.057, which is higher than 0.05, indicating no significance. Figure 6 (a) shows the parameters affecting the insertion force. The process parameters, i.e., temperature and time, have negligible impact compared with the impact of the internal diameter. The process temperature shows a relatively high impact at 170 ℃ and the process time is directly proportional to the insertion force. It can be observed that the internal diameter is a dominant factor affecting the insertion force, and the internal diameter and insertion force are inversely proportional to each other. Figure 6 (b) shows the interaction of parameters affecting the insertion force. The process times of 200 s and 300 s showed interaction at 170 ℃.

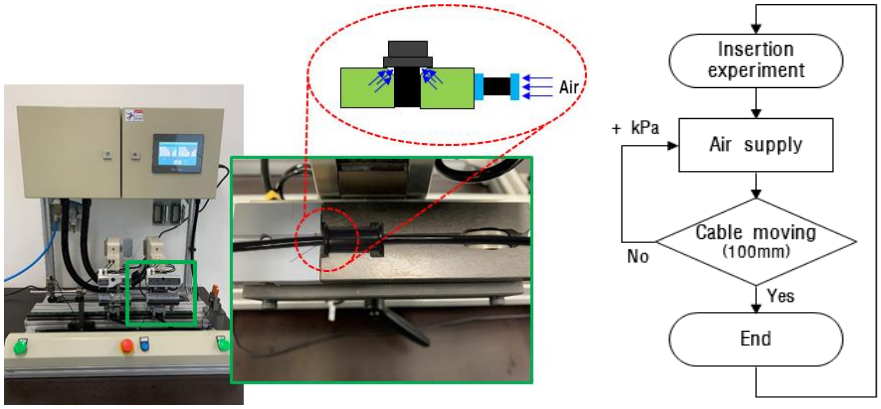

(a) Airjet insertion process equipment and schematic diagram for air supply (b) Insertion force experiment flowchart

Figure 5. Insertion force experiment and flowchart.

March - April 2020
ISSN: 0193-4120 Page No. 4547 - 4556

Table 2: Analysis of variance of insertion force

Source	DF	Adj SS	Adj MS	F-Value	P-Value
Model	26	7216.7	277.56	12.60	0.000
Linear	6	4691.9	781.99	35.50	0.000
Process temperature	2	131.1	65.53	2.97	0.057
Process time	2	530.2	265.08	12.03	0.000
Internal diameter	2	4030.7	2015.36	91.49	0.000
2-Way Interactions	12	1360.9	113.41	5.15	0.000
Process temperature*Process time	4	607.1	151.78	6.89	0.000
Process temperature*Internal diameter	4	358.1	89.51	4.06	0.005
Process time*Internal diameter	4	395.8	98.94	4.49	0.003
3-Way Interactions	8	1163.8	145.47	6.60	0.000
Process temperature*Process time* Internal diameter	8	1163.8	145.47	6.60	0.000
Error	81	1784.3	22.03		
Total	107	9000.9			

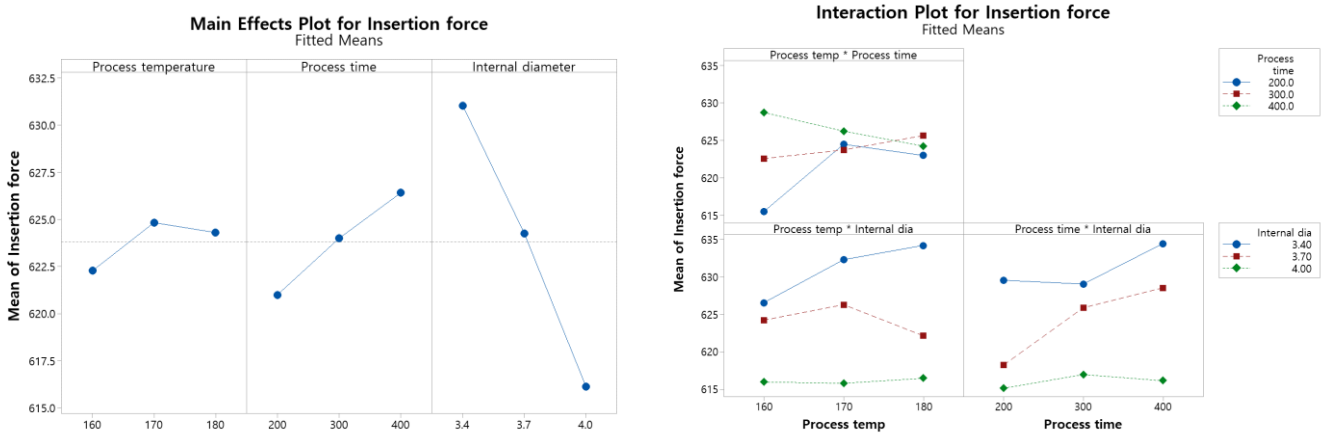

(a) Main effects plot for insertion force (b) Interaction plot for insertion force

Figure 6. Main effects plot and interaction plot for insertion force.

3.3. Separation force experiment

The schematic diagram of the separation force experiment is shown in Figure 7 (a). The grommet bonded with the cable was fixed, and the load was applied to the jig based on the longer side of the cable, until the cable was completely detached. Figure 7 (b) shows the flowchart of the separation force experiment. The separation force is based on the maximum load measured in the experiment. The experiment was repeated four times per specimen type. Table 3 shows the results of an analysis of variance of the separation force. The interaction p-value between the process temperature and the internal diameter is 0.086, which is higher than 0.05, indicating no significance. Figure 8 (a) shows the main effects of the factors affecting the separation force. Similar to the case of the insertion force, it can be observed that the impact of the process temperature and process time is insignificant compared with that of the internal diameter.

March - April 2020
ISSN: 0193-4120 Page No. 4547 - 4556

Furthermore, the process temperature and process time were directly proportional to the separation force. The internal diameter is the dominant factor affecting the separation force and the results are similar to the result in the case of the insertion force overall; however, the internal diameter of 4.0 mm has a much lower effect than the other diameters such as 3.4 mm and 3.7 mm. Figure 8 (b) shows the interaction for the separation force and the process times of 200 s and 300 s showed interactions at 170 °C.

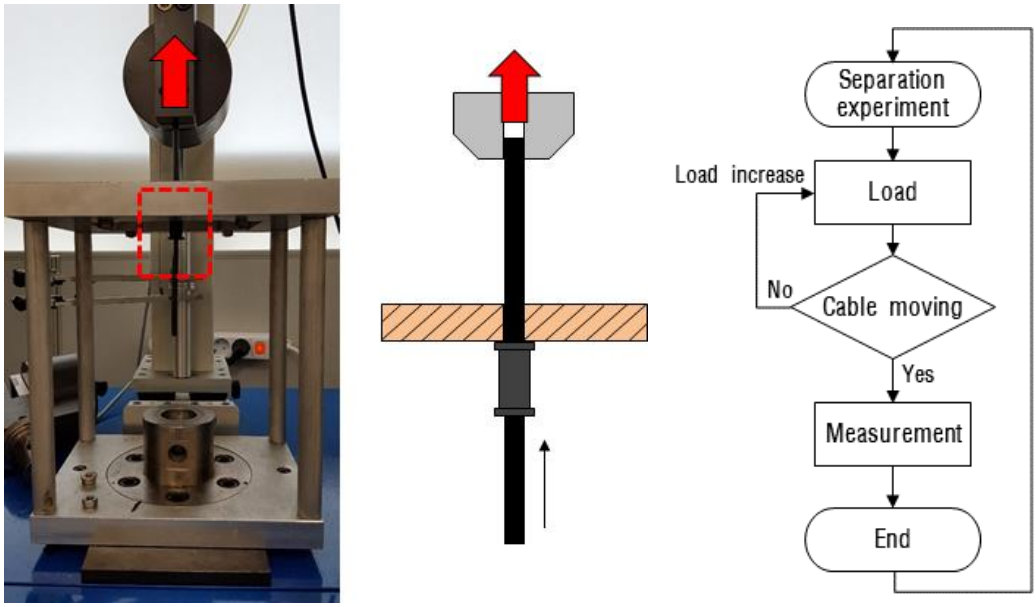

(a) Schematic diagram of separation force experiment (b) Flowchart of separation force experiment

Figure 7. Schematic diagram of separation force experiment and flowchart.

Table 3: Analysis of variance of separation force

Source	DF	Adj SS	Adj MS	F-Value	P-Value
Model	26	133.320	5.1277	49.33	0.000
Linear	6	126.433	21.0722	202.71	0.000
Process temperature	2	3.861	1.9304	18.57	0.000
Process time	2	3.645	1.8223	17.53	0.000
Internal diameter	2	118.928	59.4640	572.04	0.000
2-Way Interactions	12	4.806	0.4005	3.85	0.000
Process temperature*Process time	4	2.759	0.6898	6.64	0.000
Process temperature*Internal diameter	4	0.881	0.2202	2.12	0.086
Process time*Internal diameter	4	1.165	0.2913	2.80	0.031
3-Way Interactions	8	2.081	0.2601	2.50	0.018
Process temperature*Process time* Internal diameter	8	2.081	0.2601	2.50	0.018
Error	81	8.420	0.1040		
Total	107	141.740			

March - April 2020
ISSN: 0193-4120 Page No. 4547 - 4556

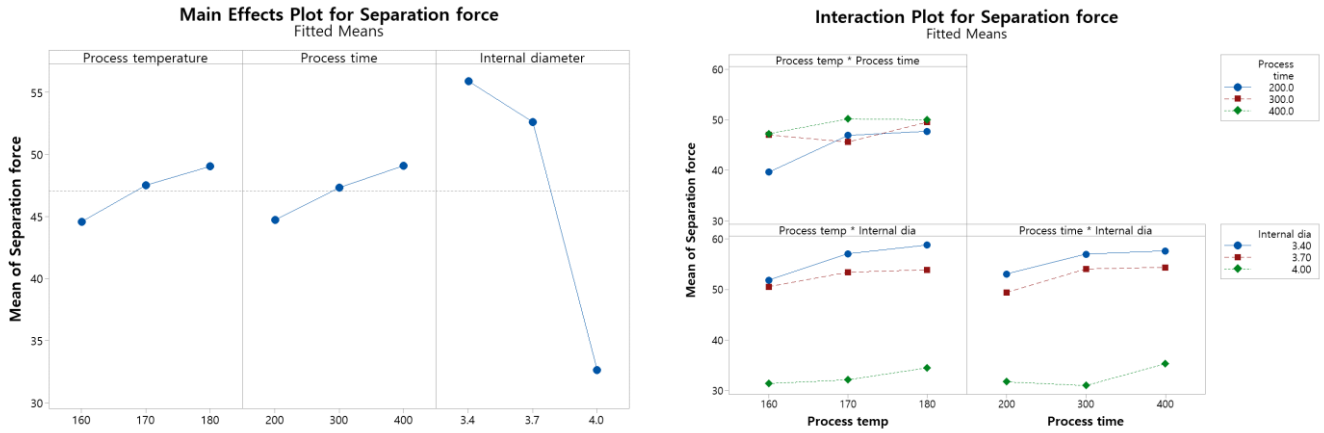

(a) Main effects plot for separation force (b) Interaction plot for separation force

Figure 8. Main effects plot and interaction plot for separation force.

4. Process Parameters and Internal Diameter Optimization

4.1. Optimization target

The optimization target for the separation force shown in Table 4 has the same acceptance criteria as commercial grommets with a load of 49.98 N. Then, the process parameters and internal diameter of the grommet inserted with the minimum pneumatic pressure among the grommets satisfying the separation force of 49.98 N or higher were derived. The weight and importance are the same between the separation force and insertion force.

Table 4: Optimization parameters

Response	Goal	Lower	Target	Upper	Weight	Importance
Separation force (N)	Target	24.5	49.98	64.68	1	1
Insertion force (kPa)	Minimum		607.0	648.0	1	1

4.2. Optimization result

Finally, the derived optimization result in Table 5 shows that the optimum grommet was the one with the internal diameter of 3.7 mm, heated at 180 ℃ for 200 s and injected. The required insertion force was 616 kPa and the separation force was 51.205 N, which was predicted to satisfy the criterion of 49.98 N or more. Figure 9 shows the optimization graph examining the insertion and separation forces according to the process parameters and internal diameter values using a response optimizer.

March - April 2020
ISSN: 0193-4120 Page No. 4547 - 4556

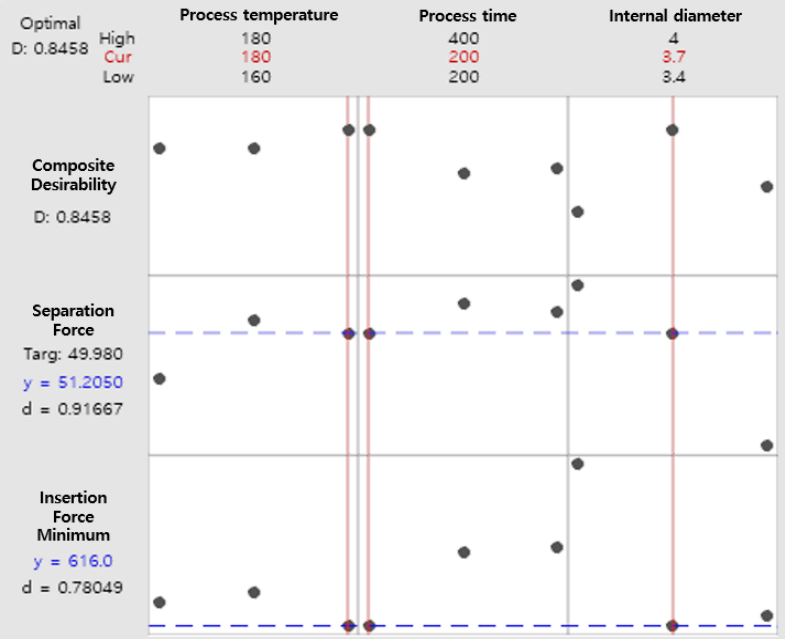

Figure 9. Parameter optimization results using response optimizers.

Table 5: Optimization result

Solution	Process temperature (℃)	Process time (s)	Internal diameter (mm)	Separation force Fit (N)	Insertion force Fit (kPa)	Composite Desirability
1	180	200	3.7	51.205	616	0.845841

5. Conclusion

In this study, the process parameters and internal diameter of the grommet made of EPDM rubber were optimized for the application of the airjet insertion method. Tensile strength and elongation percentage experiments were conducted to analyze the change in the elastic force, which is a physical property of rubber, according to the process temperature and process time. Based on the results, the elastic modulus was derived and the trend of elastic modulus change according to the process parameters was examined. In addition, insertion force and separation force experiments were conducted with the grommet specimens fabricated according to the process parameters and internal diameters, and the effects of the process parameters and structural parameter on the grommet were analyzed. Finally, the optimization results of the process parameters and internal diameter were derived through the full factorial design of DOE.

Consequently, it was confirmed that, as for the parameters affecting the insertion and separation forces, the internal diameter had a more dominant effect than the process parameters, i.e., temperature and time.

The process parameters tended to be directly proportional to the insertion and separation forces, whereas the internal diameter tended to be inversely proportional to the forces. However, when the internal diameter increased to 4.0 mm, the insertion and separation forces did not satisfy the criteria, indicating no significance in the result.

In future studies, more precise optimization results need to be derived through a more detailed classification of the internal diameter, which is the dominant factor affecting the insertion and separation forces.

March - April 2020
ISSN: 0193-4120 Page No. 4547 - 4556

6. Acknowledgment

This paper was supported by the Human Resource Training Program(S2755803) for business-related research and development of Ministry of SMEs and Startups in 2019.

This paper was supported by the Regional Specialized Industry Development R&D Convergence Program(P0005112) for business-related research and development of Ministry of SMEs.

References

[1] Kondyurin A. EPDM rubber modified by nitrogen plasma immersion ion implantation. Materials. 2018 Apr;11(5):657.

[2] Abou-Helal MO, El-Sabbagh SH. A study on the compatibility of NR–EPDM blends using electrical and mechanical techniques. Journal of Elastomers and Plastics. 2005 Oct;37:319-346.

[3] Ginic-Markovic M, Choudhury NR, Dimopoulos M, Matisons J. Adhesion between polyurethane coating and EPDM rubber compound. Journal of Adhesion Science and Technology. 2004 Jan;18(5):575-596.

[4] Kim, YS, Jeon ES, Hwang ES. Effects of injection molding process conditions on physical properties of EPDM using design of experiment method. MATEC Web of Conferences. 2018 Jan;167 1-6.

[5] Maamoun A, Xue Y, Elbestawi M, Veldhuis S. Effect of selective laser melting process parameters on the quality of Al alloy parts: Powder characterization, density, surface roughness, and dimensional accuracy. Materials. 2018 Nov;11(12) 2343.

[6] Ismail H, Shaari SM. Curing characteristics, tensile properties and morphology of palm ash/halloysite nanotubes/ethylene-propylene-diene monomer (EPDM) hybrid composites. Polymer Testing. 2010 Oct;29(7)872-878.

[7] Gatos KG, Thomann R, Karger-Kocsis J. Characteristics of ethylene propylene diene monomer rubber/organoclay nanocomposites resulting from different processing conditions and formulations. Polymer International. 2004 Jun;53 1191-1197.

[8] Ismail H, Pasbakhsh P, Ahmad Fauzi MN, Bakar AA. Morphological, thermal and tensile properties of halloysite nanotubes filled ethylene propylene diene monomer (EPDM) nanocomposites. Polymer Testing. 2008 Oct;27(7):841-850.

[9] Zhao Q, Li X, Gao J. Aging of ethylene–propylene–diene monomer (EPDM) in artificial weathering environment. Polymer Degradation and Stability. 2007 Oct;92(1)1841-1846.

[10] Kwak SB, Choi NS, Choi YJ, Shin SM. Nondestructive characterization of degradation of EPDM rubber for automotive radiator hoses. Key Engineering Materials. 2006 Jan;326-328 565-568.

[11] Kim, YS, Jeon ES, Hwang ES. Optimization of Shape Design of Grommet through Analysis of Physical Properties of EPDM Materials. Applied Sciences. 2019 Jan;9(1) 133.